Accepted Manuscript online: 2023-01-27 Article published online: 2023-02-15

Exploring Indeno[2,1-*c*]fluorene Antiaromatics with Unsymmetrical Disubstitution and Balanced Ambipolar Charge-Transport Properties

Himanshu Sharma[a]
Ankita[b]
Pooja Bhardwaj[a]
Upendra Kumar Pandey[*b]
Soumyajit Das[*a]

[a] Department of Chemistry, Indian Institute of Technology Ropar, Rupnagar, Punjab 140001, India
[b] Department of Electrical Engineering, School of Engineering, Shiv Nadar Institution of Eminence, Gautam Buddha Nagar, Uttar Pradesh 201314, India
[*] upendra.pandey@snu.edu.in; chmsdas@iitrpr.ac.in

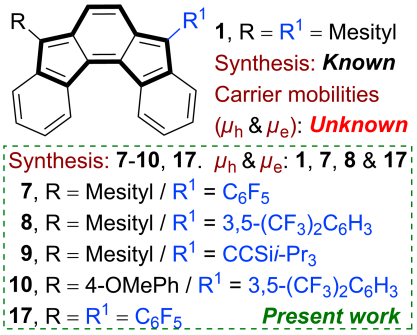

Received: 16. 10. 2022
Accepted after revision: 25.01.2023
DOI: 10.1055/a-2020-0308; Art ID: OM-2022-10-0043-OA

Abstract Unsymmetrically disubstituted antiaromatic indenofluorene (IF), in comparison to aromatic pentacene counterpart with unsymmetrical disubstitution, was rare in the literature until our recent report on indeno[1,2-*b*]fluorene and indeno[2,1-*a*]fluorene. Described herein is a straightforward access to unsymmetrically disubstituted indeno[2,1-*c*]fluorenes bearing mesityl at one apical carbon and C_6F_5, 3,5-$(CF_3)_2C_6H_3$, and CCS*i*-Pr_3 at the other apical carbon, including 4-methoxyphenyl/3,5-$(CF_3)_2C_6H_3$ push/pull substitution at the apical carbons with appreciable orbital density, and a previously unknown symmetrically C_6F_5-disubstituted [2,1-*c*]IF. The electronic properties of the unsymmetrical derivatives lie halfway in between the two symmetrical counterparts, while the 4-methoxyphenyl derivative showed the smallest HOMO–LUMO energy gap and near-infrared absorption with intramolecular charge transfer character. Single-crystal analyses showed 1D-columnar stacks for the unsymmetrical motif with the C_6F_5 units co-facially π-stacked with the IF core, whereas symmetrically C_6F_5-disubstituted [2,1-*c*]IF, with a low-lying LUMO, showed intermolecular π–π stacks between the IFs that resulted in good electron mobility ($\mu_e = 8.66 \times 10^{-3}\,cm^2 \cdot V^{-1} \cdot s^{-1}$) under space charge limited current measurements. Importantly, balanced ambipolar charge-transport behaviour could be extracted for an IF series with symmetrical/unsymmetrical substitutions, in comparison to its π-contracted pentalene congener.

Key words: indenofluorenes, indacene, polycyclic antiaromatics, ambipolar charge-transport, charge-carrier mobility, optoelectronic properties

Introduction

Fully conjugated indeno[2,1-*c*]fluorene is a structural isomer of the five antiaromatic indenofluorene (IF) regioisomers.[1,2] Studies on [2,1-*c*]IF revealed its slightly helical backbone with a *para*-quinoidal arrangement of the *as*-indacene subunit, and negligible diradical contribution in the singlet ground state, affording three stable symmetrically disubstituted derivatives **1**, **2** and **3** (Figure 1b).[1] In comparison to the isomeric indeno[1,2-*b*]fluorene[2a] with a *para*-quinodimethane (*p*-QDM) arrangement in the *s*-indacene subunit (shown in bold, Figure 1a), the *as*-indacene (shown in bold, Figure 1b) embedded [2,1-*c*]IF is less documented,[2e] despite showing a smaller HOMO–LUMO energy gap[1] and potential application as an electron acceptor in bulk heterojunctions.[3] Majority of the studies conducted with the [2,1-*c*]IF revealed that its electronic, redox, and solid-state properties can be tuned by elongating the pentacyclic backbone by quinoidal fluorenofluorene[4] modification (*as*-indacene subunit not retained) or by condensing the benzene unit in the form of benzo-fused [2,1-*c*]IF derivatives **4**, **5** and **6**, where the *as*-indacene subunit is retained.[5] However, unsymmetrical var-

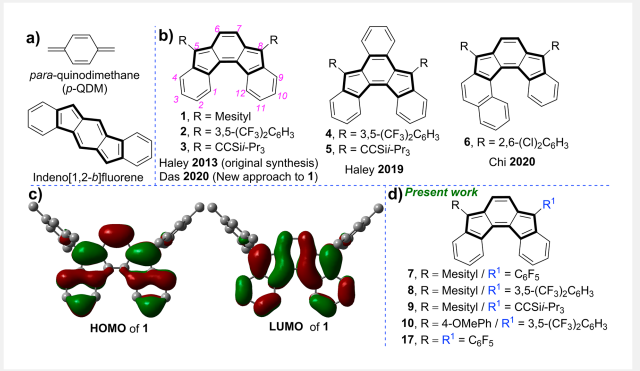

Figure 1 a) *p*-QDM-embedded indeno[1,2-*b*]fluorene. b) *p*-QDM-embedded isomeric [2,1-*c*]IF derivatives **1**–**6**. c) Frontier molecular orbital profiles of **1**. d) Target unsymmetrical [2,1-*c*]IFs **7**–**10** and the unknown symmetrical **17**.

iation of both substituents at the apical carbon centers to tune the electronic and solid-state properties was never explored.[1,2e]

Lack of access to the unsymmetrically disubstituted IFs[1,2,5] is likely due to the limitation of a controlled nucleophilic addition[6] of aryl/ethynyl groups to the benzo-fused diketone precursor, which has hampered exploration of unsymmetrically disubstituted IFs. Lately, two unsymmetrically disubstituted IF regioisomers were reported by us with tunable antiaromaticity.[7] We had reported a new synthesis approach to **1**,[8] and further to a (4 n + 2)π *s*-indacenodifluorene. Inspired by the general route for unsymmetrically 6,13-disubstituted pentacene molecules for various applications[9] and considering appreciable molecular orbital density at the apical carbons of **1** (Figure 1c) or related *as*-indacene[10] that suggested possibility to tune the electronic properties of [2,1-*c*]IFs by apical elongation, including the non-availability of unsymmetrically 5,8-disubstituted [2,1-*c*]IFs, we envisaged to extend our synthetic approach[8] as a general route to access the yet inaccessible unsymmetrically 5,8-disubstituted [2,1-*c*]IF scaffolds **7**, **8**, **9** and **10** (Figure 1d), and a previously unknown[1] symmetrically disubstituted [2,1-*c*]IF **17**.

The aryl or ethynyl groups like C_6F_5,[11] [3,5-bis(trifluoromethyl)phenyl],[12] and [(triisopropylsilyl)ethynyl][13] are chosen due to their proven ability to sterically protect the apical carbons and the electron-accepting nature.[14] It was also anticipated that replacing weakly electron-donor mesityl of **8** with 4-methoxyphenyl for **10** may offer improved push–pull character. Additionally, the [2,1-*c*]IF scaffold was known[1] but its charge-carrier mobility was unknown, and it was speculated to have poor performance due to its U-shape hindering π–π stacks.[2e] Inspired by the reports of ambipolar charge transport of [1,2-*b*]IF[2f] with symmetrical disubstitution, and use of [1,2-*b*]IF for single-molecule conductance studies,[2h] herein, we report the syntheses of four unsymmetrical [2,1-*c*]IFs **7**–**10** and one symmetrical [2,1-*c*]IF **17** including their characterization by both experimental and computational[15] approaches, and the charge-carrier mobilities of **1**, **7**, **8** and **17** were experimentally investigated using the space charge limited current (SCLC) method.

Results and Discussion

C_6F_5-disubstituted [1,2-*b*]IF is an ambipolar material,[16] which motivated us to synthesize **17** as it was not reported earlier.[1] Treating our pre-synthesized aldehyde **11**[8] with pentafluorophenylmagnesium bromide (C_6F_5MgBr) under ambient conditions afforded **12** (Scheme 1), which was converted to **13** using $BF_3{\cdot}Et_2O$-mediated Friedel–Crafts (FC) alkylation. The Suzuki reaction between **13** and (2-formylphenyl)boronic acid gave aldehyde **14**, which was treated further with C_6F_5MgBr to afford the carbinol **15**. Treatment of crude **15** with $BF_3{\cdot}Et_2O$ gave the dihydro-precursor **16** in 62% yield over two steps. Dichloro-5,6-dicyano-1,4-benzoquinone (DDQ)-mediated oxidative dehydrogenation of **16** at 100 °C in 1,2-dichloroethane afforded **17** in 94% yield.

We then turned our attention to synthesize the unsymmetrically disubstituted [2,1-*c*]IF derivatives **7**, **8** and **9**. Nucleophilic addition of Grignard/ethynyllithium reagents like C_6F_5MgBr, [3,5-bis(trifluoromethyl)phenyl]magnesium bromide, and [(triisopropylsilyl)ethynyl]lithium (TIPSELi) to our pre-synthesized aldehyde **18**[8] afforded the three different carbinols **19**, **21** and **23**, respectively (Scheme 2). These carbinols were further treated with $BF_3{\cdot}Et_2O$ to afford the dihydro-precursors **20**, **22** and **24**, respectively. Conversion of **23** to **24** was accompanied by partial formation of **9**. Nevertheless, DDQ-mediated oxidative dehydrogenation of **20**, **22** and crude **24** proceeded smoothly (in different solvents) to afford **7**, **8** and **9**, respectively, which are confirmed by NMR spectroscopy (see the Supporting Information, SI), including single-crystal X-ray analyses for **7**, **9** and **17** (vide infra).

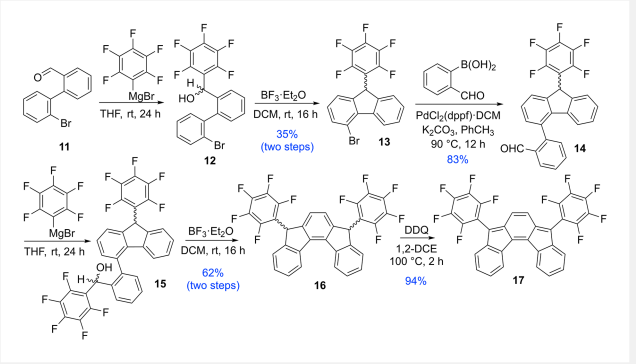

Scheme 1 Synthesis of new symmetrically disubstituted [2,1-*c*]IF **17**.

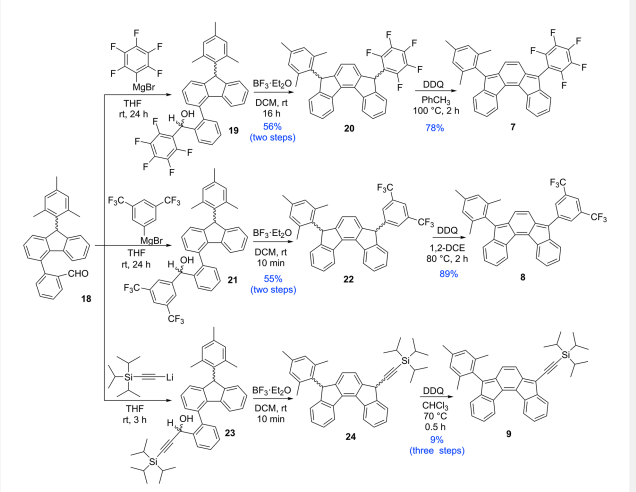

Scheme 2 Syntheses of the unsymmetrically disubstituted [2,1-*c*]IFs **7**, **8** and **9**.

Unlike our steric approach to synthesize [1,2-*b*]IF that required mesityl as a bulky substituent,[7] the current approach can be used to attach less bulky donors (e.g. 4-methoxyphenyl) to afford push–pull dyes. Compound **10** was synthesized using the analogous synthesis approach (Scheme 3) that started with a nucleophilic addition of (4-methoxyphenyl)magnesium bromide to aldehyde **11** to afford **25**. Treating **25** with triflic acid at room temperature gave **26**, which underwent a Suzuki cross-coupling reaction with (2-formylphenyl)boronic acid to give **27** in 75% yield. Nucleophilic addition of 3,5-$(CF_3)_2C_6H_3$-MgBr to **27** followed by $BF_3{\cdot}OEt_2$ treatment afforded the dihydro-precursor **29** in 61% yield over two steps. Finally, treatment of **29** with excess of DDQ in toluene afforded **10** with donor and acceptor[14] substituents in moderate yield.

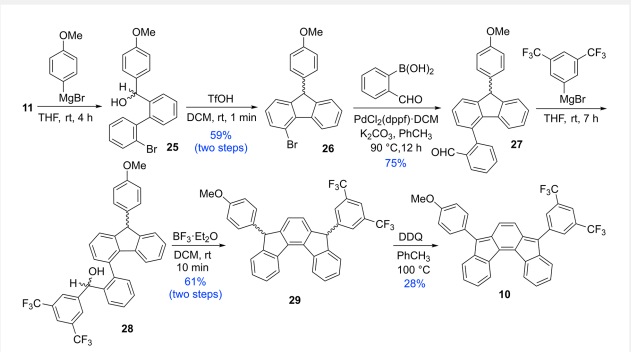

Scheme 3 Synthesis of a push–pull disubstituted [2,1-*c*]IF **10**.

Single crystals for **7**, **9** and **17** were grown successfully, and analyzed. The X-ray crystallographic analysis showed a nearly planar [2,1-*c*]IF backbone for **7** (Figure 2a, CCDC 2 117 444) with the outer benzenoid ring (near to C_6F_5) twisted by 7.0° from the average plane of the cyclopenta[*c*]fluorene subunit. Compound **9** (Figure 2c, CCDC 2 117 445) packs in two independent arrangements with 12.9° and 13.6° twist angles, suggesting subtle *P*/*M*-like helicity with a very small 0.48 kcal/mol *P*/*M*-interconversion barrier (see SI).[1] The mesityl group is found to be near-orthogonally oriented to the [2,1-*c*]IF backbone (dihedral angle 86.9 – 89.7° for **7** and **9**), while the other aryl/ethynyl groups suggest a

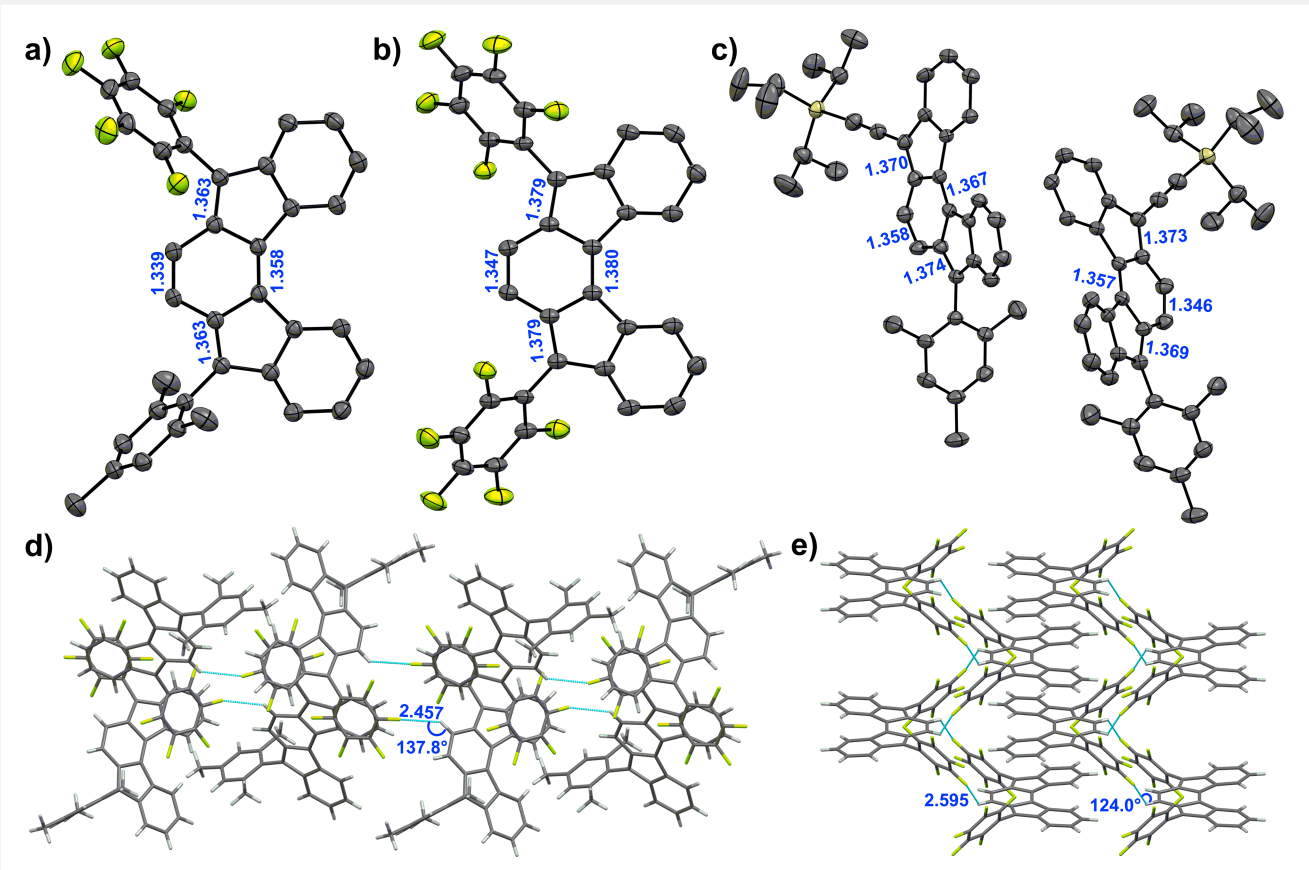

Figure 2 ORTEP drawing of a) **7**, b) **17**, and c) **9** (left: *P*-isomer; right: *M*-isomer) at 30% probability level (hydrogen omitted), with the C=C bond distances (in Å) of *p*-quinodimethane unit are shown. The packing motifs for d) **7** and e) **17** showing the intermolecular F···H–C_{sp^2} hydrogen bonds (in Å) and their ($\angle C_{sp^2}$–H···F) angles.

better π-delocalization trend on moving from C_6F_5 in **7** (a reduced dihedral angle ~52.6°) to TIPSE in **9** (co-planar). The bond lengths of the [2,1-*c*]IF backbones clearly suggested a *para*-quinoidal arrangement of the *as*-indacene[1,7,8] (C=C double bond distances are shown in Figure 2a, 2b and 2c) for all the derivatives, including homogeneous C_{sp^2}–C_{sp^2} bond-length distributions in the outer benzenoid rings for **7**, **9** and **17**, which clearly implies benzene aromaticity for outer six-membered rings.[1,7]

X-ray crystallographic analysis of **7** has shown several close contacts in the solid state (Figure S39) with intermolecular non-covalent interactions between $C_{(9)}$–$C_{(5)}$ (3.238 Å, π–π) and $C_{(4)}$–$F_{(4)}\cdots C_{(15)}$ (3.137 Å, C – F···π) centers of the C_6F_5 and [2,1-*c*]IF π-rings, including two intermolecular $C_{(20)}$–$H_{(20)}\cdots C_{(18)}$ and $C_{(9)}$–$H_{(9)}\cdots C_{(34)}$ C – H···π interactions (2.859 Å) between the [2,1-*c*]IF backbones and strong intermolecular C_{sp^2}–$F_{(2)}\cdots H_{(34)}$–C_{sp^2} hydrogen bonding interaction measuring 2.457 Å (the value is less than the sum of the van der Waals radii of F and H = 2.67 Å)[17] with $\angle C_{sp^2}$–H···F = 137.8°, affording a herringbone-like packing arrangement (Figure S39) with a 1D columnar stack featuring the C_6F_5 unit partly, co-facially, π-stacking (3.238 Å) with the outer ring of IF (Figure 2d). The hydrogen-bond distance and bond angle meet the geometrical requirements for intermolecular hydrogen bonding interactions.[18] The H···F–C_{sp^2} hydrogen bond interaction is critical in the formation of a supramolecular assembly for calixphyrins[19] or antiaromatic isophlorins[20]; however, from the perspective of diradicaloid polycyclic hydrocarbons,[11] including antiaromatic IFs,[2,16,21] H···F–C hydrogen bonding interactions received seldom attention. In comparison to **7**, symmetrical **17** (CCDC 2117446) displayed weaker intermolecular $F_{(3)}\cdots H_{(8)}$–$C_{(8)}$ (2.595 Å, $\angle C_{sp^2}$–H···F = 124.0°) hydrogen bonding interactions in a 1D columnar arrangement featuring two IF backbones π-stacking at 3.574 Å, co-facially, at about a point of inversion (Figure 2e), implying strong intermolecular π–π interaction (Figure S40).

All new [2,1-*c*]IF derivatives displayed strong absorbance in the higher energy (UV-vis) region and a broad absorption in the lower energy (visible) region extending to 800 nm (Figure 3), except for **10** that has extended to 840 nm in the near-infrared (NIR) region. Symmetrical diarylation/ethynylation at the 5/8 positions to tune optoelectronic properties[1] seems logical by the calculated HOMO/LUMO plots (Figure 1c), which show considerable orbital density at the apical carbons. It is thus expected that unsymmetrical aryl/aryl or aryl/ethynyl disubstitution could be a realistic step to fine-tune the optoelectronic properties. The source of the broad low energy absorption band was predicted by the time-dependent density functional theory (DFT) calculations as π→π* electronic transitions, originating from an admixture of the HOMO→LUMO and HOMO-1→LUMO transitions in the singlet closed-shell ground state (Table S1 – S5 in SI). The absorption profiles were also characteristically

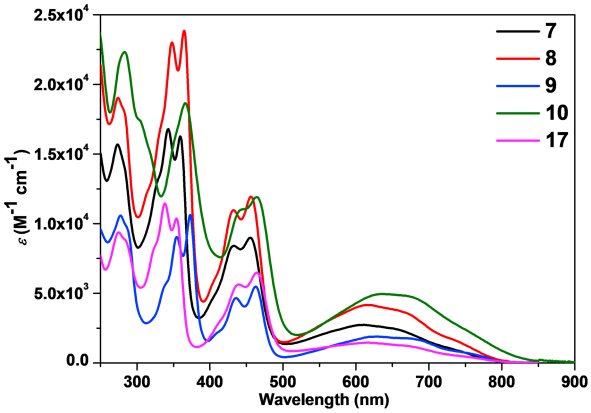

Figure 3 UV-vis-NIR absorption plots of the new [2,1-*c*]IFs in $CHCl_3$.

similar to the symmetrically 5,8-disubstituted [2,1-*c*]IF derivatives,[1] with **17** being the newest entry with λ_{abs}^{max} = 616 nm (theoretical λ_{max} = 746 nm, oscillator strength (*f*) = 0.1056; Table S5). To our expectation, the absorption maxima for **8** are found to lie in between those of **1** and **2**, and similarly for **9** (between **1** and **3**) as well as **7** (between **1** and **17**).

The red-shift in the absorption band (λ_{max} = 610 nm, ε = 2780 $M^{-1}\cdot cm^{-1}$) with theoretical *f* = 0.1052 (719 nm, Table S1) for **7** in the visible region, in comparison to **1**, can be attributed to some electronic communication between the C_6F_5 and [2,1-*c*]IF π-rings due to the decrease in dihedral angle (observed for crystals). This observation is also supported by the DFT studies with a reduced dihedral angle ca. 52 – 53° for **7**, in comparison to the orthogonally oriented mesityl group. The lower energy absorption maximum is further red-shifted for **8** (λ_{max} = 615 nm, ε = 4170 $M^{-1}\cdot cm^{-1}$; *f* = 0.1197 at 724 nm, Table S2), suggesting a better π-delocalization between the 3,5-bis(trifluoromethyl)phenyl and [2,1-*c*]IF π-rings due to a further reduction of the dihedral angle (ca. 44 – 46° for **8** at B3LYP/6 – 31 G(d,p)), including stronger electron-withdrawing effect. Further improvement in the electronic communication between the coplanar TIPSE and the [2,1-*c*]IF core in **9** is reflected by the more red-shifted absorption (λ_{max} = 625 nm, ε = 1880 $M^{-1}\cdot cm^{-1}$; *f* = 0.1516 at 742 nm, Table S3) and a smaller optical HOMO–LUMO energy gap of 1.52 eV than that of **7** (E_g^{opt} = 1.56 eV) or **8** (E_g^{opt} = 1.55 eV). Compound **10** showed the smallest optical energy gap (E_g^{opt} = 1.47 eV) with a red-shifted low-energy absorption band (λ_{max} = 640 nm, ε = 4940 $M^{-1}\cdot cm^{-1}$; *f* = 0.1708 at 755 nm, Table S4), with the absorption tail reaching the NIR region. A weak but non-negligible blue-shift (~10 nm) of the low-energy wavelength maximum for **10** was noticed when changing the solvent from polar $CHCl_3$ to non-polar hexane (Figure S36), suggesting an intramolecular charge transfer (ICT) character due to

a better push–pull interaction between the 4-methoxyphenyl (electron donor) and 3,5-$(CF_3)_2C_6H_3$ (electron acceptor)[14] substituents through the *as*-indacene backbone. However, no obvious change in absorption profile was noticed when changing the solvent polarity for **8** (Figure S35), indicating negligible ICT interaction due to a weakly electron-donating mesityl group. Compounds **7**, **8**, **9**, **10** and **17** are found to be non-emissive, a common trait for antiaromatic [2,1-*c*]IF.[22]

The unsymmetrical [2,1-*c*]IFs accept two electrons quasi-reversibly, and they are quasi-reversibly oxidized to a radical cation, and further, quasi-reversibly to the dications (Figure 4, Table 1). It was noticed that if current was swept through the second reduction for **9** and **17**, and second oxidation for **7**, **8** and **9**, new peaks (as bumps) appeared on their return during the cathodic and anodic scans. Such peaks were not observed if the current was not swept past the first reduction and oxidation potentials (Figure S37b in SI), indicating likely formation of some reactive species during the second reduction and oxidation. The first half-wave ($E_{1/2}$) oxidation potential, obtained from differential pulse voltammogram peak values (Figure S37a), at $E^{ox1}_{1/2}$ = 0.66 V (vs. ferrocene/ferrocenium (Fc/Fc^+) for **7** is the highest among the unsymmetrical motifs, and **8** and **9** appeared at $E^{ox1}_{1/2}$ = 0.63 V and 0.55 eV, respectively, while **10** showed the smallest value at $E^{ox1}_{1/2}$= 0.43 V. Compound **9** appears to be a comparatively better electron acceptor with a low first half-wave reduction potential at $E^{red1}_{1/2}$ = −1.32 V than **7** or **10** with $E^{red1}_{1/2}$ = −1.36 V and **8** with $E^{red1}_{1/2}$ = −1.39 V. The estimated electrochemical HOMO–LUMO energy gaps (E^{ec}_g) are 1.54 eV for **10**, 1.56 eV for **9**, 1.75 eV for **8**, and 1.76 eV for **7**. Symmetrical **17** could be oxidized at a high potential of $E^{ox1}_{1/2}$ = 0.84 V and reduced at a much lower reduction potential of $E^{red}_{1/2}$ = −1.16 V with an estimated E^{ec}_g = 1.71 eV.

The trend of optical and electrochemical energy gaps for **7**, **8**, **9**, **10** and **17** is consistent with the theoretical HOMO–LUMO energy gaps (Table 1). The low-lying LUMO of **17** (−3.80 eV) and improved solid-state packing interaction suggested its potential as a good electron transporter; however, the amphoteric redox waves[23] observed for these new IFs prompted us to investigate both hole and electron transport behaviors for a [2,1-*c*]IF series: **1**, **7** and **17**. Since reports suggest that possibly the device architecture in solar cells may not appropriately fit with the transistor mobility,[24] the

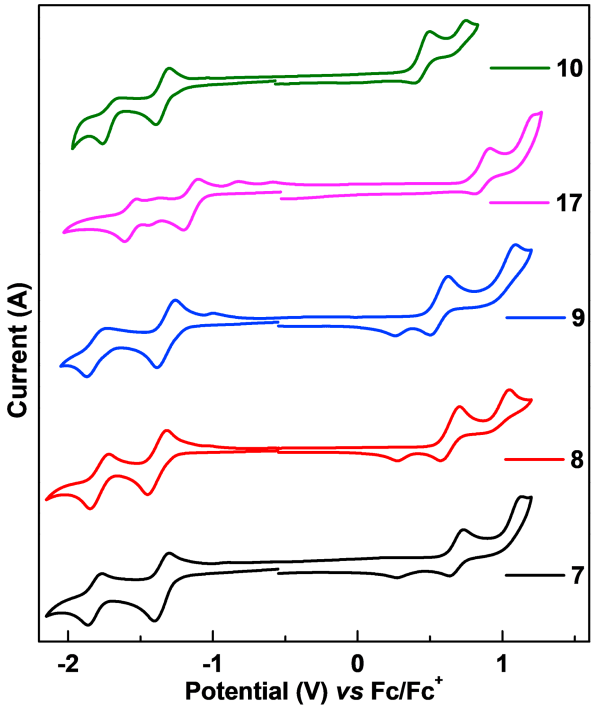

Figure 4 Cyclic voltammogram of the new [2,1-*c*]IF derivatives in CH_2Cl_2.

Table 1 Summary of photophysical and electrochemical data for **7**, **8**, **9**, **10** and **17**[a]

Comp.	$E^{red}_{1/2}$ [V]	$E^{ox}_{1/2}$ [V]	HOMO [eV]	LUMO [eV]	E^{ec}_g [eV]	λ_{abs} [nm]	ε [$M^{-1}\cdot cm^{-1}$]	E^{opt}_g [eV]	E^{DFT}_g [eV]
7	−1.36 −1.83	0.66 1.04	−5.35	−3.59	1.76	610, 454, 431, 359, 342, 272	2780, 9040, 8410, 16330, 16870, 15740	1.56	2.18
8	−1.39 −1.78	0.63 0.97	−5.33	−3.58	1.75	615, 456, 432, 364, 347, 273	4170, 11930, 10960, 23880, 22990, 19000	1.55	2.15
9	−1.32 −1.82	0.55 0.99	−5.24	−3.65	1.59	625, 462, 435, 372, 354, 277	1880, 5490, 4620, 10590, 9000, 10560	1.52	2.03
10	−1.36 −1.73	0.43 0.68	−5.16	−3.62	1.54	640, 464, 445, 366, 283	4940, 11910, 11040,18650, 22330	1.47	2.02
17	−1.16 −1.37 −1.58	0.84 1.12	−5.51	−3.80	1.71	616, 464, 439, 354, 338, 274	1450, 6470, 5640, 10390, 11450, 9350	1.53	2.11

[a]λ_{abs} = absorption maxima; ε = molar extinction coefficient for the corresponding absorption maximum; $E_{1/2}$ = half-wave potentials (first and second) for oxidative and reductive waves against the Fc/Fc^+ couple; HOMO = −(4.8 + E^{onset}_{ox}) and LUMO = −(4.8 + E^{onset}_{red}); E^{ec}_g = electrochemical HOMO–LUMO energy gap; E^{opt}_g = optical HOMO–LUMO energy gap calculated from the onset absorption wavelength; E^{DFT}_g = theoretical HOMO–LUMO energy gap.

more relevant[25] SCLC method was adopted by us to measure the charge-carrier mobility (vide infra), in order to find the potential for these new molecules as new semiconductors for organic electronic devices.

The charge-carrier mobilities of compounds **1**, **7**, **8** and **17** were determined from the current–voltage characteristic of devices having hole (ITO/PEDOT:PSS/**1**, **7**, **8** and **17**/MoO_3/Ag) and electron-only (ITO/SnO_2/**1**, **7**, **8** and **17**/Al) architectures. The charge-carrier mobility is determined from fitting the *J*–*V* characteristics with a semi-log plot for compounds **1**, **7**, **8** and **17** using the modified Mott–Gurney equation given by Murgatroyd[26]:

$$J = \frac{9}{8}\mu\varepsilon_r\varepsilon_o\frac{V^2}{d^3}\exp\left(0.891\cdot\gamma\cdot\sqrt{V/d}\right) \quad (1)$$

where *J* is measured as current density, ε_o is the permittivity of free space (8.86×10^{-14} F/cm), ε_r is relative dielectric constant of the material, *V* is applied voltage, *d* is the thickness of the active layer of the material, μ is mobility, and γ is the fitting parameter representing the strength of the field dependence on mobility. The extracted mobilities of the compounds are summarized in Table 2.

Table 2 Summary of SCLC hole and electron mobilities

Compounds	Mobility ($cm^2\cdot V^{-1}\cdot s^{-1}$)		
	Hole ($\times10^{-3}$)	Electron ($\times10^{-3}$)	μ_e/μ_h
1	1.27 ± 0.23	2.20 ± 1.37	1.73
7	1.80 ± 0.82	7.26 ± 5.12	4.03
8	1.47 ± 0.30	3.82 ± 3.04	2.60
17	1.64 ± 0.50	8.66 ± 2.89	5.28

The *J*–*V* characteristics for compounds **1**, **7**, **8** and **17** are shown in Figure 5. From the SCLC mobilities shown in Table 2, it is evident that the known compound **1**, and the new compounds **7**, **8** and **17**, showed ambipolarity for charge-carrier transport where for both hole and electrons, the order of the observed charge-carrier mobility is same. Overall, for a device application, a material having balanced electron and hole mobility is preferred.[27] In these reported compounds, the closeness order for the balanced ambipolar compound is found to be in the order **17** < **7** < **8** < **1**, which seems reasonable considering appreciable intermolecular interactions observed in the solid state for **7** and **17** resulting in better charge-transport properties. On the other hand, compound **1** with bulkier mesityl substituents lacks any appreciable intermolecular π–π interactions,[1,2e] unlike **17**, affording relatively low SCLC mobilities than those of **17** or **7**. Nonetheless, the charge-transport behavior of unsymmetrical **7** lies nearly halfway in between its symmetrical counterparts **1** and **17** (Table 2). The observed higher electron mobility for compound **17** can be attributed to its favorable energy level alignment in electron-only devices with aluminum and a better intermolecular π–π interaction when compared with compounds **1** and **7**.

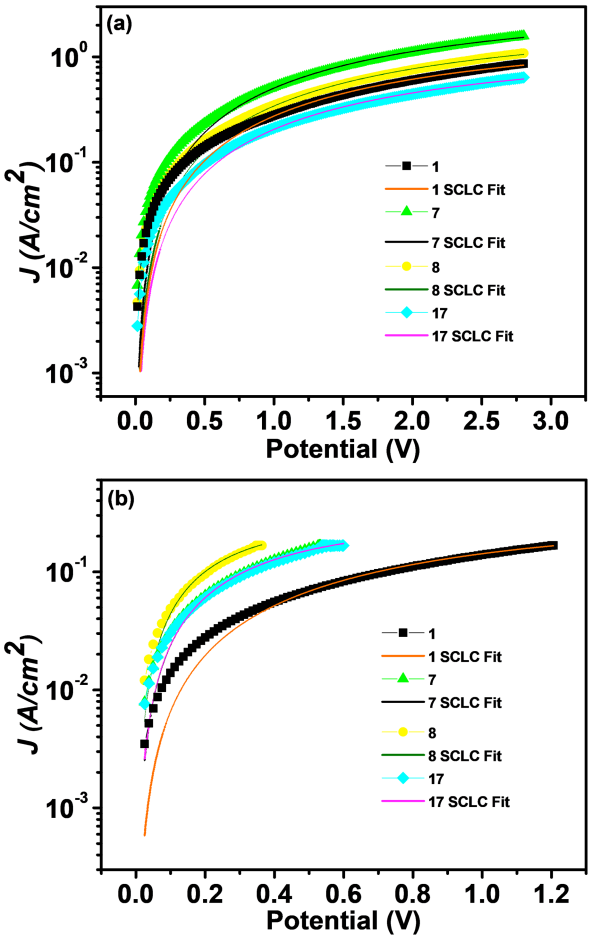

Figure 5 *J*–*V* characteristics in the semi-log plot used for extracting (a) hole and (b) electron mobilities using modified the Mott–Gurney SCLC equation for compounds **1**, **7**, **8** and **17**.

It is worth noting that SCLC mobilities of organic semiconductor thin films are much lower in comparison to the field-effect mobility, usually within 10^{-6} to 10^{-4} $cm^2\cdot V^{-1}\cdot s^{-1}$.[28] Although sulfur-embedded small polycyclic aromatic system was reported to show good SCLC hole mobility (8.72×10^{-2} $cm^2\cdot V^{-1}\cdot s^{-1}$),[25a] hydrocarbon motifs like antiaromatic diareno-pentalene showed low hole-carrier mobility (4.37×10^{-4} $cm^2\cdot V^{-1}\cdot s^{-1}$) under the SCLC method.[29] Considering [2,1-*c*]IF as a benzo-interpositioned[30] pentalene system, our studies on the symmetrical or unsymmetrical [2,1-*c*]IFs **1**, **7**, **8** and **17** π-systems revealed an order of magnitude greater charge-carrier mobility for both holes and electrons. Moreover, a balanced ambipolar charge-transport behavior could be extracted for the first time. This suggests that [2,1-*c*]IF-based antiaromatic systems could be

a useful candidate for applications in organic optoelectronic devices, and high-performance materials with proper structural modifications are in the scope of our future studies.

Conclusions

In summary, unsymmetrically 5,8-disubstituted [2,1-*c*]IFs **7**, **8**, **9** and a push–pull disubstituted **10**, and a symmetrically 5,8-disubstituted [2,1-*c*]IF **17** were reported for the first time using a synthetic approach that has the potential to generate strongly polarized [2,1-*c*]IFs, as well as heteroatom-modified[31] isoelectronic [2,1-*c*]IF in the near future. X-ray crystallographic analyses revealed improved solid-state properties for **7** and **17**, including shorter intermolecular F···H–C_{sp^2} hydrogen bonding interactions in unsymmetrical **7** (2.457 Å, 137.8°) than that was observed for symmetrical **17** (2.595 Å, 124.0°), and intermolecular π–π interactions. The electronic properties of the unsymmetrical **7**, **8** and **9** lie halfway in between two symmetrically disubstituted [2,1-*c*]IF counterparts. The HOMO–LUMO energy gap of **10** was found to be the smallest due to the ICT character arising from the push–pull effect of apical substituents, implying possibilities to further lowering the energy gap by substituent modification.

Our report of convenient access to fully conjugated [2,1-*c*]IFs bearing desired substituents with balanced ambipolar charge-transport properties for **1**, **7**, **8** and **17** in the order of 10^{-3} $cm^2 \cdot V^{-1} \cdot s^{-1}$ could open the gateway to previously inaccessible apically extended antiaromatic materials for diverse applications in organic optoelectronics devices. To the best of our knowledge, this is the first systematic study of charge-carrier mobility of antiaromatic [2,1-*c*]IFs bearing symmetrical (**1**, **17**) and unsymmetrical (**7**) disubstitution comprising two particular substituents (mesityl and C_6F_5). Our work distinctly showed the potential of [2,1-*c*]IF scaffolds as efficient charge-transporting materials, one of the fundamental requirements for efficient organic electronic devices, which is in contrast to earlier prediction.[2e] Further exploration of the [2,1-*c*]IF derivatives for optoelectronic applications with a focus on transistors and solar cells alongside the unsymmetrical [1,2-*b*]IF[7] regioisomers is currently being explored.

Experimental Section

General Information. All reagents and chemicals were obtained from commercial sources and used as received. Silica gel (100 – 200 mesh) was used for column chromatography. NMR spectra, in solution, were recorded on a JEOL JNM ECS-400 spectrometer at 298 K. The following abbreviations were used to explain the multiplicities: s = singlet, d = doublet, t = triplet, and m = multiplet. ^1H and ^{13}C chemical shifts (δ) are reported in ppm relative to the residual $CHCl_3$ (^1H: 7.26 ppm, ^{13}C: 77.16 ppm) reference. Single-crystal analyses were done on a CMOS-based Bruker D8 Venture PHOTON 100 diffractometer equipped with a INCOATEC micro-focus source with graphite monochromated Mo Kα radiation (λ = 0.71 073 Å) operating at 50 kV and 30 mA. High-resolution mass spectra (HRMS) were recorded using electron spray ionization (ESI) methods on Waters (XEVO G2-XS QTOF) mass spectrometer. UV-vis-NIR absorption spectra were recorded as solution, on a JASCO V-770 spectrophotometer. Cyclic voltammetry measurements were performed in dry dichloromethane (DCM) at room temperature under a nitrogen atmosphere on a CHI-1110C instrument electrochemical analyzer with a three-electrode cell, using Bu_4NPF_6 as the supporting electrolyte, Ag/AgCl as the reference electrode, Pt disk as the working electrode, and Pt wire as the counter electrode at 50 mV/s scan rate. The potential was externally calibrated against the ferrocene/ferrocenium couple. Melting points were determined using a BIBBY-SMP30 melting point analyzer.

Procedures

***4-Bromo-9-(perfluorophenyl)-9H-fluorene* (13).** To a dry THF solution (10 mL) of pre-synthesized compound **11** (246 mg, 0.94 mmol), (perfluorophenyl)magnesium bromide (0.5 M solution in diethylether, 3.8 mL, 1.88 mmol) was added dropwise under nitrogen and the solution was stirred for 24 h at room temperature. The formation of product was monitored by a thin-layer chromatography (TLC), and once the conversion to **12** is complete, a saturated solution of ammonium chloride (20 mL) was added to quench the reaction. The solvent was removed under reduced pressure and the residue was extracted with DCM (3 × 50 mL). The combined organic layer was dried over sodium sulfate and the solvent was removed under vacuum to afford crude **12** as brown solid (415.8 mg). Crude **12** (415.8 mg) was further dissolved in dry DCM (15 mL) and treated with 0.1 mL of boron trifluoride·diethyl etherate ($BF_3 \cdot Et_2O$) under nitrogen to perform an intra-molecular ring-closure (FC) reaction. After stirring overnight, a saturated aqueous NH_4Cl solution (20 mL) was added to the reaction mixture and extracted with DCM (3 × 50 mL). The solvent was dried over sodium sulfate, and was evaporated to dryness. The crude mixture obtained was subjected to silica gel column chromatography (hexanes) to afford the title product **13** as white solid (136 mg, 35% yield over two steps). R_f = 0.4 (hexanes). Mp: 124 – 125 °C. ^1H NMR (400 MHz, $CDCl_3$): δ 8.66 (d, *J* = 8.0 Hz, 1 H), 7.60 (d, *J* = 7.9 Hz, 1 H), 7.49 (t, *J* = 7.6 Hz, 1 H), 7.36 (m, 1 H), 7.28 (d, *J* = 7.5 Hz, 1 H), 7.23 (d, *J* = 7.5 Hz, 1 H), 7.14 (t, *J* = 7.7 Hz, 1 H), 5.46 (s, 1 H). $^{13}C\{^1H\}$ NMR (100 MHz, $CDCl_3$): δ 146.8, 144.4, 140.4, 139.5, 133.2, 128.3, 128.3 127.9, 124.0,

123.1, 117.3, 42.8. HRMS (ESI) *m/z*: $[M - H]^+$ Calcd for $C_{19}H_7BrF_5$ 408.9651, found 408.9691.

***2-(9-(Perfluorophenyl)-9H-fluoren-4-yl)benzaldehyde* (14).** A solution of **13** (122 mg, 0.29 mmol), (2-formylphenyl)boronic acid (89 mg, 0.59 mmol), anhydrous K_2CO_3 (205 mg, 1.48 mmol) and dry toluene (6 mL) was degassed by sparging with N_2 for 0.5 h in an oven-dried thick-walled glass tube. $PdCl_2$(dppf)·DCM complex (24 mg, 10 mol%) was added thereafter, and the reaction vessel was sealed. The reaction mixture was then heated under stirring at 90 °C for 12 h. After cooling to room temperature, water was added and the mixture was extracted with DCM (3 × 50 mL) and the combined organic extracts were dried over Na_2SO_4. After removal of the solvent, the crude was subjected to column chromatography on silica gel (hexanes : EtOAc, 95 : 5) as an eluent to afford **14** as white solid (108 mg, 83% yield). R_f = 0.47 (hexanes : EtOAc = 95 : 5). Mp: 135 – 136 °C. ^{1}H NMR (400 MHz, $CDCl_3$): δ 9.82 (m, 1 H), 8.15 (m, 1 H), 7.77 (m, 1 H), 7.66 (t, *J* = 7.3 Hz, 1 H), 7.57 – 7.47 (m, 1 H), 7.41 – 7.35 (m, 2 H), 7.32 – 7.27 (m, 1 H), 7.25 (s, 1 H), 7.20 (m, 1 H), 7.06 (t, *J* = 7.6 Hz, 1 H), 6.55 (dd, *J* = 7.8, 3.2 Hz, 1 H), 5.52 (d, *J* = 6.9 Hz, 1 H). ^{13}C{^{1}H} NMR (100 MHz, $CDCl_3$): δ 192.0, 191.9, 144.7, 144.6, 144.3, 144.2, 140.4, 139.5, 139.3, 134.5, 134.4, 134.2, 134.1, 133.1, 133.0, 131.1, 130.8, 130.4, 128.8, 128.1, 128.0, 127.8, 127.7, 127.6, 127.5, 127.3, 127.2, 124.4, 124.3, 124.2, 122.7, 42.5. HRMS (ESI) *m/z*: $[M + H]^+$ Calcd for $C_{26}H_{14}OF_5$ 437.0965, found 437.0988.

***5,8-Bis(perfluorophenyl)-5,8-dihydroindeno[2,1-c]fluorene* (16).** Under a nitrogen atmosphere, in 10 mL dry THF solution of **14** (79 mg, 0.18 mmol), (perfluorophenyl)magnesium bromide (0.5 M solution in diethylether, 1.1 mL, 0.54 mmol) was added dropwise. The mixture was stirred at room temperature for 24 h. After removal of the solvent, the crude compound was quenched with NH_4Cl (20 mL) and extracted into DCM (3 × 40 mL), washed with brine, and dried over anhydrous sodium sulfate. The starting material **14** was consumed, so the crude **15** (131 mg, HRMS *m/z*: [M – H$^+$] Calcd for $C_{32}H_{13}OF_{10}$ 603.0807, found 603.0805) was used for the next step without purification. To the solution of crude brown solid **15** (125 mg, 0.206 mmol) in anhydrous DCM (10 mL) at room temperature, 0.1 mL of BF_3·Et_2O was added dropwise under nitrogen, and the reaction mixture was stirred for 16 h at room temperature. Once the reaction was complete, as monitored by TLC, a saturated aqueous NH_4Cl (10 mL) solution was added to the reaction mixture and extracted with DCM (3 × 30 mL). The organic layer was dried over anhydrous Na_2SO_4, filtered, and concentrated under reduced pressure. Product **16** was purified from the crude mixture using a silica gel column (hexanes) as white solid, as mixture of stereoisomers (66 mg, 62% yield over two steps). R_f = 0.66 (hexanes). Mp: 222 – 223 °C. ^{1}H NMR (400 MHz, $CDCl_3$): δ 8.60 (d, *J* = 7.9 Hz, 2 H), 7.63 – 7.51 (m, 2 H), 7.46 – 7.32 (m, 4 H), 7.18 (d, *J* = 4.5 Hz, 2 H), 5.56 (s, 1 H), 5.51 (s, 1 H). ^{13}C{^{1}H} NMR (100 MHz, $CDCl_3$): δ 145.8, 145.4, 145.2, 145.1, 141.2, 136.9, 128.0, 127.8, 127.7, 124.6, 124.2, 124.1, 123.1, 43.0. HRMS (ESI) *m/z*: $[M - H]^+$ Calcd for $C_{32}H_{11}F_{10}$ 585.0701, found 585.0718.

***5,8-Bis(perfluorophenyl)indeno[2,1-c]fluorene* (17).** 2,3-Dichloro-5,6-dicyano-1,4-benzoquinone (18.6 mg, 0.08 mmol, 2.5 equiv.) was added as solid to the degassed 1,2-dichloroethane (1 mL) solution of **16** (19.2 mg, 0.03 mmol) under nitrogen in a glass tube, and the resultant solution was heated at 100 °C under sealed conditions for 2 h. The reaction mixture was cooled to room temperature, and then run through a short silica gel plug eluting with hexanes to obtain the title product. Following a pentane wash, pure compound **17** was obtained as green solid (18 mg, 94% yield). R_f = 0.63 (hexanes). Mp: 274 – 275 °C. ^{1}H NMR (400 MHz, $CDCl_3$, 25 °C) δ 8.08 – 8.00 (m, 2 H), 7.22 – 7.12 (m, 4 H), 6.85 (dd, *J* = 6.9, 1.9 Hz, 2 H), 6.29 (s, 2 H). ^{13}C{^{1}H} NMR (100 MHz, $CDCl_3$, 25 °C): δ 144.0, 140.0, 138.9, 135.9, 129.9, 127.9, 126.1, 122.3, 122.0. ^{19}F NMR (376 MHz, $CDCl_3$, 25 °C) δ −135.69 (s), −152.46 (d, *J* = 21.9 Hz), −160.63 (t, *J* = 22.6 Hz). HRMS (ESI) *m/z*: $[M + H]^+$ Calcd for $C_{32}H_{11}F_{10}$ 585.0701, found 585.0690.

***5-Mesityl-8-(perfluorophenyl)-5,8-dihydroindeno[2,1-c]fluorene* (20).** To a 10 mL dry THF solution of **18** (93 mg, 0.24 mmol) under a nitrogen atmosphere, dropwise addition of pentafluorophenylmagnesium bromide (0.5 M in diethylether, 2.87 mL, 1.44 mmol) was done and the mixture was stirred at room temperature for 24 h. The reaction mixture was quenched with NH_4Cl (20 mL), and extracted with DCM (3 × 40 mL) after evaporation of THF. After drying the solvent mixture over sodium sulfate, the solvents were removed to isolate crude alcohol **19** as dark brown solid (373.8 mg, HRMS (ESI) *m/z*: $[M - H]^+$ Calcd for $C_{35}H_{24}OF_5$ 555.1747, found 557.1757), which (370 mg, 0.66 mmol) was further dissolved in dry DCM (10 mL) at room temperature and treated with 0.1 mL of BF_3·Et_2O and the reaction mixture was stirred for 16 h at room temperature under N_2. After complete consumption of carbinol **19**, as monitored by TLC, a saturated aqueous NH_4Cl solution (10 mL) was added to the reaction mixture and extracted with DCM (3 × 30 mL). The organic layer was dried over anhydrous Na_2SO_4, filtered, and the solvent was subsequently removed under reduced pressure. The residue was purified by silica gel column chromatography (hexanes) to afford the title product **20** (72.6 mg, 56% yield over two steps) as white solid, as mixture of stereoisomers. R_f = 0.5 (hexanes). Mp: 70 – 71 °C. ^{1}H NMR (400 MHz, $CDCl_3$): δ 8.66 – 8.59 (m, 2 H), 7.59 – 7.49 (m, 2 H), 7.39 – 7.27 (m, 4 H), 7.16 – 7.10 (m, 2 H), 7.04 – 7.02 (m, 1 H), 6.67 – 6.65 (m, 1 H), 5.60 – 5.54 (m, 2 H), 2.70 – 2.68 (m, 3 H), 2.29 – 2.27 (m, 3 H), 1.08 – 1.06 (m, 3 H). ^{13}C{^{1}H} NMR (100 MHz, $CDCl_3$): δ 149.3, 148.9, 148.6, 148.5,

145.2, 145.1, 144.8, 144.2, 141.7, 141.0, 140.9, 138.0, 137.9, 137.8, 136.7, 136.6, 136.5, 136.4, 134.3, 130.8, 130.7, 128.9, 127.9, 127.5, 127.4, 126.8, 124.6, 124.5, 124.0, 124.1, 123.9, 123.8, 123.0, 122.9, 122.8, 122.5, 50.1, 50.0, 43.0, 21.9, 21.8, 21.0, 18.8, 18.7. HRMS (ESI) *m/z*: $[M + H]^+$ Calcd for $C_{35}H_{24}F_5$ 539.1798, found 539.1776.

***5-(3,5-Bis(trifluoromethyl)phenyl)-8-mesityl-5,8-dihydroindeno[2,1-c]fluorene* (22).** [3,5-bis(trifluoromethyl)-phenyl]magnesium bromide was firstly prepared from 1-bromo-3,5-bis(trifluoromethyl)benzene (0.6 mL, 5 equiv., 3.5 mmol), Mg (101.7 mg, 6 equiv., 4.2 mmol) and catalytic I_2 in freshly distilled THF (5 mL). Afterwards, anhydrous 20 mL THF solution of aldehyde **18** (271 mg, 0.697 mmol)) was added to the freshly prepared [3,5-bis(trifluoromethyl)-phenyl]magnesium bromide at room temperature under a N_2 atmosphere, and the resulting solution was stirred at room temperature for 24 h. After addition of aqueous NH_4Cl (20 mL), the organic phase was separated, and the aqueous phase was extracted with DCM (3 × 40 mL) and washed with brine solution. Upon evaporating off the solvent, the crude **21** (511.6 mg) (HRMS (ESI) *m/z*: $[M - H]^+$ Calcd for $C_{37}H_{27}OF_6$ 601.1966, found 601.1977) was obtained as yellow oil which was used without purification. Crude **19** (466.8 mg, 0.77 mmol) in anhydrous DCM (10 mL), at room temperature, was treated with 0.1 mL of $BF_3{\cdot}Et_2O$ and stirred for 10 min. The reaction was quenched by 10 mL aqueous NH_4Cl solution, and extracted with DCM (3 × 30 mL). The solvent was dried over anhydrous sodium sulfate, filtered, and was removed under vacuum to afford crude **22**, which was purified by column chromatography (silica, hexanes) to give white solid **22** as a mixture of stereoisomers (232 mg, 55% yield over two steps). R_f = 0.55 (hexanes). Mp: 115 – 116 °C. ^{1}H NMR (400 MHz, $CDCl_3$): δ 8.66 – 8.61 (m, 2 H), 7.77 – 7.75 (m, 1 H), 7.58 – 7.51 (m, 4 H), 7.37 – 7.29 (m, 4 H), 7.12 – 7.02 (m, 3 H), 6.67 – 6.65 (m, 1 H), 5.59 (s, 1 H), 5.25 – 5.23 (m, 1 H), 2.70 – 2.69 (m, 3 H), 2.29 – 2.27 (m, 3 H), 1.09 – 1.05 (m, 3 H). ^{13}C{^{1}H} NMR (100 MHz, $CDCl_3$): δ 149.3, 148.6, 147.3, 147.1, 146.7, 146.2, 145.3, 145.2, 141.6, 141.5, 140.9, 137.9, 137.8, 136.7, 136.5, 134.2, 132.6, 132.3, 131.9, 131.6, 130.8, 130.7, 129.0, 128.9, 128.7, 128.6, 128.0, 127.6, 127.6, 127.5, 126.8, 125.5, 125.4, 124.7, 124.6, 124.1, 124.0, 123.9, 123.8, 123.7, 123.3, 123.2, 122.0, 121.2, 54.1, 53.9, 50.1, 50.0, 21.9, 21.9, 21.8, 21.0, 20.9, 18.8, 18.6. HRMS (ESI) *m/z*: $[M + H]^+$ Calcd for $C_{37}H_{27}F_6$ 585.2017, found 585.2070.

***5-Mesityl-8-(perfluorophenyl)indeno[2,1-c]fluorene* (7).** DDQ (34 mg, 0.14 mmol, 2 equiv.) was added to degassed solution of precursor **20** (40 mg, 0.07 mmol) in toluene (2 mL), and the reaction mixture was heated to 100 °C for 2 h. The progress of the reaction was monitored by TLC and stopped after 2 h, followed by purification by silica gel column chromatography (hexanes) to afford the final compound **7** as green solid (31 mg, 78% yield). R_f = 0.50 (hexanes). Mp: 246 – 247 °C. ^{1}H NMR (400 MHz, $CDCl_3$, 25 °C): δ 8.10 (d, *J* = 6.4 Hz, 1 H), 8.03 (d, *J* = 7.5 Hz, 1 H), 7.17 (m, 3 H), 7.06 (t, *J* = 7.4 Hz, 1 H), 6.97 (s, 2 H), 6.88 (d, *J* = 5.9 Hz, 1 H), 6.67 (d, *J* = 7.2 Hz, 1 H), 6.21 (s, 2 H), 2.35 (s, 3 H), 2.15 (s, 6 H). ^{13}C{^{1}H} NMR (100 MHz, $CDCl_3$, 25 °C): δ 147.2, 146.1, 144.1, 140.8, 139.3, 138.1, 137.9, 136.9, 136.7, 136.3, 135.6, 129.8, 129.4, 129.3, 128.3, 127.7, 126.9, 125.8, 125.7, 125.6, 122.9, 122.6, 121.5, 120.2, 21.3, 20.3. ^{19}F NMR (376 MHz, $CDCl_3$, 25 °C) δ −135.99 (d, *J* = 21.9 Hz), −153.51 (d, *J* = 20.4 Hz), −161.09 (t, *J* = 23.4 Hz). HRMS (ESI) *m/z*: $[M + H]^+$ Calcd for $C_{35}H_{22}F_5$ 537.1642, found 537.1631.

***5-(3,5-Bis(trifluoromethyl)phenyl)-8-mesitylindeno[2,1-c]fluorene* (8).** DDQ (69.8 mg, 0.30 mmol, 1.2 equiv.) was added to dry 1,2-dichloroethane (1 mL) solution of precursor **22** (150 mg, 0.25 mmol) to carry out the oxidative dehydrogenation reaction. The reaction mixture was then heated to 80 °C for 2 h, and the progress was monitored by TLC. After 2 h, the solvent was removed in vacuo and the crude residue was purified on silica gel column chromatography (hexanes) to afford the pure compound **8** as green solid (133 mg, 89% yield). R_f = 0.51 (hexanes). Mp: 197 – 198 °C. ^{1}H NMR (400 MHz, $CDCl_3$, 25 °C): δ 8.17 – 8.12 (m, 1 H), 8.07 (d, *J* = 7.4 Hz, 1 H), 7.96 (s, 2 H), 7.90 (s, 1 H), 7.25 – 7.04 (m, 5 H), 6.97 (s, 2 H), 6.71 (d, *J* = 7.2 Hz, 1 H), 6.49 (d, *J* = 9.3 Hz, 1 H), 6.27 (d, *J* = 9.4 Hz, 1 H), 2.35 (s, 3 H), 2.15 (s, 6 H). ^{19}F NMR (376 MHz, $CDCl_3$, 25 °C) δ −62.77 (s). ^{13}C{^{1}H} NMR (100 MHz, $CDCl_3$, 25 °C): δ 146.4, 146.1, 144.5, 140.6, 138.4, 137.9, 137.8, 137.0, 136.9, 136.5, 136.3, 136.2, 132.4, 132.1, 129.7, 129.5, 129.4, 129.3, 128.3, 127.4, 127.2, 126.0, 125.8, 124.7, 123.0, 122.5, 122.0, 121.6, 121.0, 119.5, 21.3, 20.3. HRMS (ESI) *m/z*: $[M + H]^+$ Calcd for $C_{37}H_{25}F_6$ 583.1860, found 583.1824.

***Triisopropyl((8-mesitylindeno[2,1-c]fluoren-5-yl)ethynyl)silane* (9).** A flame-dried round-bottomed flask equipped with a stir bar was charged with TIPS-acetylene (0.52 mL, 2.32 mmol, 5.0 equiv.). Freshly distilled THF (5 mL) was then introduced into the flask and the resulting solution was cooled to 0 °C under an inert atmosphere. A 1.6 M solution of n-butyllithium in hexanes (5.0 equiv.) was then added and the reaction mixture was stirred at 0 °C. After 30 min, the reaction was mixed with a solution of **18** (180 mg, 0.46 mmol) in THF. After complete consumption of carbonyl **18**, the reaction mixture was quenched with saturated aqueous solution of ammonium chloride (20 mL) and diluted with ethyl acetate (30 mL). The layers were separated and the organic layer was washed with brine. The extracts were dried over sodium sulfate, filtered, and was concentrated in vacuo to afford crude product **23** as dark brown solid (451 mg, HRMS (ESI) *m/z*: $[M + H]^+$ Calcd for $C_{40}H_{47}OSi$ 571.3396, found 571.3273). To the solution of crude **23** (431 mg, 0.75 mmol) in anhydrous DCM (10 mL) at room temperature, $BF_3{\cdot}Et_2O$ (0.1 mL) was added dropwise under

nitrogen, and the reaction mixture was stirred for 10 min at room temperature. Completion of the reaction was monitored by TLC (partial formation of **9** was observed in TLC, likely due to air oxidation), and the mixture was extracted with DCM/water to afford **24** (78 mg, including the partly dehydrogenated **9**), which was used directly for the next step. A chloroform (10 mL) solution of the crude **24** was treated with DDQ (38 mg, 0.16 mmol, 1.2 equiv.) for 0.5 h at 70 °C. The final compound **9** was obtained as green gummy solid (23 mg, 9% yield over three steps) after purification of the crude reaction residue by silica gel (hexanes) column chromatography. R_f = 0.44 (hexanes). Mp: 104 – 105 °C. ^{1}H NMR (400 MHz, $CDCl_3$, 25 °C): δ 8.00 (d, *J* = 7.3 Hz, 2 H), 7.29 (d, *J* = 7.1 Hz, 1 H), 7.21 (dd, *J* = 11.3, 4.1 Hz, 1 H), 7.17 (dd, *J* = 7.3, 6.2 Hz, 1 H), 7.11 (t, *J* = 7.2 Hz, 1 H), 7.04 (t, *J* = 7.2 Hz, 1 H), 6.96 (s, 2 H), 6.73 (d, *J* = 9.2 Hz, 1 H), 6.67 (d, *J* = 7.2 Hz, 1 H), 6.25 (d, *J* = 9.2 Hz, 1 H), 2.35 (s, 3 H), 2.13 (s 6 H), 1.16 – 1.15 (m, 21 H). ^{13}C{^{1}H} NMR (100 MHz, $CDCl_3$, 25 °C): δ 146.1, 145.9, 145.0, 142.8, 139.6, 138.5, 137.7, 136.9, 136.8, 136.6, 135.6, 129.7, 129.4, 128.3, 127.2, 127.0, 125.6, 125.2, 123.3, 122.3, 122.0, 121.8, 121.0, 107.4, 101.6, 21.2, 20.3, 18.8, 11.4. HRMS (ESI) *m/z*: $[M + H]^+$ Calcd for $C_{40}H_{43}Si$ 551.3134, found 551.3112.

***4-Bromo-9-(4-methoxyphenyl)-9H-fluorene* (26).** To a dry THF solution (10 mL) of pre-synthesized compound **11** (850 mg, 3.26 mmol) was added (4-methoxyphenyl)magnesium bromide (prepared from 1-bromo-4-methoxybenzene (0.49 mL 3.91 mmol) and magnesium turning (142 mg, 5.86 mmol) in dry THF (5 mL)) and the solution was stirred for 4 h at room temperature. Then the reaction was quenched with a saturated aqueous solution of NH_4Cl and extracted with EtOAc. The extract was washed with brine and dried over Na_2SO_4 to afford crude **25** as brown solid (1263 mg). Crude **25** (1249 mg) was further dissolved in dry DCM (10 mL) and treated with TfOH (1 drop) under a N_2 atmosphere to perform an intra-molecular ring-closure (FC) reaction. After stirring for 1 min, appropriate amount of silica gel was added to the mixture, and the solvent was evaporated in vacuo. The residue was purified by column chromatography on silica gel (hexanes) to afford the title product **26** as white solid (669 mg, 59% yield in two steps). R_f = 0.3 (hexanes). Mp: 56 – 57 °C. ^{1}H NMR (400 MHz, $CDCl_3$): δ 8.64 (d, *J* = 7.8 Hz, 1 H), 7.54 (d, *J* = 8.0 Hz, 1 H), 7.44 (m, 1 H), 7.36 – 7.29 (m, 2 H), 7.24 (d, *J* = 7.5 Hz, 1 H), 7.09 (t, *J* = 7.7 Hz, 1 H), 6.99 (d, *J* = 8.7 Hz, 2 H), 6.82 (d, *J* = 8.6 Hz, 2 H), 5.01 (s, 1 H), 3.78 (s, 3 H). ^{13}C{^{1}H} NMR (100 MHz, $CDCl_3$): δ 158.8, 151.2, 148.7, 140.2, 139.2, 133.1, 132.3, 129.5, 128.2, 128.0, 127.1, 125.2, 124.3, 123.5, 116.9, 114.3, 55.3, 53.9. HRMS (ESI) *m/z*: $[M - H]^+$ Calcd for $C_{20}H_{14}Obr$ 349.0228, found 349.0218.

***2-(9-(4-Methoxyphenyl)-9H-fluoren-4-yl)benzaldehyde* (27).** A solution of **26** (669 mg, 1.90 mmol), (2-formylphenyl)boronic acid (571 mg, 3.81 mmol), anhydrous K_2CO_3 (1.32 g, 9.52 mmol) and dry toluene (8 mL) was degassed by sparging with N_2 for 0.5 h in an oven-dried thick-walled glass tube. $PdCl_2$(dppf)·DCM complex (155 mg, 10 mol%) was added thereafter, and the reaction vessel was sealed. The reaction mixture was then heated under stirring at 90 °C for 12 h. After cooling to room temperature, water was added and the mixture was extracted with EtOAc (3 × 50 mL) and the combined organic extracts were dried over Na_2SO_4. After removal of the solvent, the crude was subjected to column chromatography on silica gel (hexanes : DCM, 1 : 1 as eluent) to afford **27** as white solid (537 mg, 75% yield). R_f = 0.8 (hexanes : DCM = 1 : 1). Mp: 55 – 56 °C. ^{1}H NMR (400 MHz, $CDCl_3$): δ 9.92 – 9.86 (m, 1 H), 8.17 (m, 1 H), 7.80 – 7.73 (m, 1 H), 7.69 – 7.62 (m, 1 H), 7.55 (m, 1 H), 7.42 – 7.37 (m, 1 H), 7.33 (m, 1 H), 7.29 (d, *J* = 7.5 Hz, 1 H), 7.23 (d, *J* = 7.3 Hz, 1 H), 7.17 (m, 1 H), 7.09 – 6.99 (m, 3 H), 6.86 (dd, *J* = 8.8, 2.3 Hz, 2 H), 6.55 (dd, *J* = 7.3, 2.1 Hz, 1 H), 5.07 – 5.06 (m, 1 H), 3.80 (s, 3 H). ^{13}C{^{1}H} NMR (100 MHz, $CDCl_3$): δ 192.2, 192.1, 158.7, 148.9, 148.8, 144.9, 140.1, 139.0, 134.3, 134.3, 134.2, 134.0, 133.4, 133.3, 132.4, 131.0, 131.0, 129.7, 129.5, 129.4, 128.6, 127.5, 127.4, 127.4, 127.2, 126.9, 126.9, 125.4, 125.3, 125.2, 122.3, 114.3, 114.3, 55.3, 53.6, 53.6. HRMS (ESI) *m/z*: $[M + H]^+$ Calcd for $C_{27}H_{21}O_2$ 377.1542, found 377.1542.

***5-(3,5-Bis(trifluoromethyl)phenyl)-8-(4-methoxyphenyl)-5,8-dihydroindeno[2,1-c]fluorene* (29).** Under a nitrogen atmosphere, in 10 mL dry THF solution of **27** (162 mg, 0.43 mmol), (3,5-bis(trifluoromethyl)phenyl)magnesium bromide (prepared from 1-bromo-3,5-bis(trifluoromethyl)-benzene (0.37 mL, 2.15 mmol) and magnesium turning (63 mg, 2.58 mmol) in dry THF (5 mL)) was added dropwise. The mixture was stirred at room temperature for 7 h. After removal of the solvent, the crude compound was quenched with NH_4Cl (20 mL) and extracted into EtOAc (3 × 40 mL), washed with brine, and dried over anhydrous sodium sulfate. The starting material **27** was consumed, so the crude **28** (367 mg, HRMS *m/z*: $[M - H^+]$ Calcd for $C_{35}H_{23}O_2F_6$ 589.1602, found 589.1603) was used for the next step without purification. To the solution of crude brown solid **28** (361 mg, 0.61 mmol) in anhydrous DCM (10 mL) at room temperature, 0.2 mL of BF_3·Et_2O was added dropwise under nitrogen, and the reaction mixture was stirred for 10 min at room temperature. Once the reaction was complete, as monitored by thin TLC, a saturated aqueous NH_4Cl (10 mL) solution was added to the reaction mixture and extracted with DCM (3 × 30 mL). The organic layer was dried over anhydrous Na_2SO_4, filtered, and concentrated under reduced pressure. Product **29** was purified from the crude mixture using silica gel column (hexanes : EtOAc, 98 : 2) as white solid, as mixture of stereoisomers (155 mg, 61% yield over two steps). R_f = 0.4 (hexanes : EtOAc = 95 : 5). Mp: 109 – 110 °C. ^{1}H NMR (400 MHz, $CDCl_3$): δ 8.67 – 8.55 (m, 2 H), 7.77 (s,

1 H), 7.63 – 7.48 (m, 4 H), 7.42 – 7.28 (m, 4 H), 7.21 (d, J = 7.3 Hz, 1 H), 7.10 (d, J = 7.5 Hz, 1 H), 7.04 (dd, J = 8.8, 7.1 Hz, 2 H), 6.82 (d, J = 8.6 Hz, 2 H), 5.21 (s, 1 H), 5.08 (s, 1 H), 3.78 – 3.77 (m, 3 H). $^{13}C\{^1H\}$ NMR (100 MHz, $CDCl_3$): δ 158.7, 150.0, 149.9, 149.5, 149.4, 147.2, 147.0, 146.9, 146.7, 145.1, 144.9, 141.6, 141.4, 140.9, 140.9, 136.7, 136.6, 136.4, 136.2, 133.8, 133.6, 132.2, 131.9, 129.6, 129.5, 128.7, 128.0, 127.6, 127.6, 127.5, 127.3, 125.8, 125.5, 124.7, 124.6, 124.4, 124.0, 123.9, 123.8, 123.6, 122.0, 121.2, 114.3, 55.3, 54.0. HRMS (ESI) *m/z*: $[M - H]^+$ Calcd for $C_{35}H_{21}OF_6$ 571.1497, found 571.1497.

***5-(3,5-Bis(trifluoromethyl)phenyl)-8-(4-ethoxyphenyl)indeno[2,1-c]fluorene* (10).** To a solution of **29** (92 mg, 0.16 mmol) in toluene (10 mL) was added 2,3-dichloro-5,6-dicyano-*p*-benzoquinone (DDQ) (365 mg, 1.61 mmol, 10 equiv.). The reaction mixture was heated at 100 °C under sealed conditions. After 2 h, the solution was cooled to 0 °C and hydrazine monohydrate (0.5 mL) was added. The reaction mixture was purified by column chromatography on silica gel (EtOAc/hexane = 1 : 99), to give the product **10** as green solid (26 mg, 28%). R_f = 0.5 (hexanes : EtOAc = 95 : 5). Mp: 160 – 161 °C. ^1H NMR (400 MHz, $CDCl_3$, 25 °C): δ 8.14 (dd, J = 5.8, 2.9 Hz, 1 H), 8.12 – 8.06 (m, 1 H), 7.98 (s, 2 H), 7.90 (s, 1 H), 7.54 – 7.45 (m, 2 H), 7.25 – 7.23 (m, 1 H), 7.21 – 7.18 (m, 2 H), 7.18 – 7.12 (m, 3 H), 7.06 – 7.02 (m, 2 H), 6.78 (d, J = 9.5 Hz, 1 H), 6.58 (d, J = 9.3 Hz, 1 H), 3.89 (s, 3 H). $^{13}C\{^1H\}$ NMR (100 MHz, $CDCl_3$, 25 °C): δ 160.2, 145.6, 144.9, 144.4, 141.0, 138.4, 137.1, 137.0, 136.6, 136.1, 134.8, 132.7, 132.4, 132.1, 131.7, 130.8, 129.4, 129.3, 129.2, 127.5, 126.9, 126.1, 126.0, 125.8, 124.8, 123.0, 122.7, 122.1, 121.5, 120.9, 119.6, 114.4, 55.5. ^{19}F NMR (376 MHz, $CDCl_3$, 25 °C) δ −62.79 (s). HRMS (ESI) *m/z*: $[M]^+$ Calcd for $C_{35}H_{20}OF_6$ 570.1418, found 570.1418. Note: Excess of DDQ in toluene was required to convert **29** to **10** at 100 °C, likely due to a competing side reaction involving the oxidative insertion of DDQ into the C(sp3)–H bond of toluene under near-refluxing conditions, thus inhibiting the oxidizing capacity of DDQ.[32] A plausible reason of such low yield is further discussed in the appendix section of the SI (Figure S45).

Space charge limited current device fabrication. For evaluating hole and electron mobility of the compounds **1**, **7**, **8** and **17**, hole-only and electron-only devices were fabricated in the ITO/PEDOT : PSS/**1**, **7**, **8** and **17**/MoO_3/Ag and ITO/SnO_2/**1**, **7**, **8** and **17**/Al architecture, respectively. Initially, prepatterned ITO glass was substrates (12 Ω/□, Xin Yan Technology Limited, Hong Kong) were sequentially cleaned using 3% HelmanexIII soap solution, deionized water, acetone, and isopropyl alcohol in an ultrasonicator for 20 min each, respectively. Substrates were then treated with 30 min exposure to UV ozone at 50 °C. For hole-only devices, ~30 nm PEDOT : PSS layer (Sigma Aldrich) was first spin-coated on cleaned ITO substrates (4000 rpm for 65 s) followed by annealing at 150 °C for 30 min. Further, ~100 nm thick (1500 RPM for 45 s) thin films of compounds **1**, **7**, **8** and **17** were spin-coated from a 10 mg/mL solution using chloroform as the solvent. Finally, hole-only devices were then completed with thermally evaporated 5 nm of MoO_3 and 100 nm of Ag on top of the active layer. For electron-only devices, at first, SnO_2 solution was prepared by diluting 15% tin (IV) oxide colloidal solution (Alfa Aesar) in 1 : 6 by volume in deionized water. The SnO_2 solution was then spin-coated on cleaned ITO substrates at 4000 rpm for 65 s to obtain ~40 nm thick films. The spin-coated substrates were the annealed 180 °C for 1 h under ambient conditions. Furthermore, ~100 nm thick films of compounds **1**, **7**, **8** and **17** were spin-coated from the same solution as used for the hole-only devices. Lastly, 120 nm of Al was thermally evaporated at a base pressure of 3×10^{-6} mbar to complete the device. The active area of both hole- and electron-only devices was 6.6 mm^2, calculated from the overlap area of patterned ITO and top contact. J–V characteristics were measured using a Keithley 2450 source measure unit. The dielectric constant of the compounds **1**, **7**, **8** and **17** was measured using high-frequency LCR meter ZM2376 with an applied oscillation level voltage of 1 V over the frequency range 20 Hz–1 MHz.

Funding Information

S. D. gratefully acknowledges the financial support from SERB-DST India (Start-up Research Grant: SRG/2019/000401) and IIT Ropar (ISIRD grant). U. K. P. sincerely acknowledges the financial support extended by Shiv Nadar Institution of Eminence. H. S. thanks IIT Ropar for senior research fellowship. Ankita thanks Shiv Nadar IoE for research fellowship. The central research facilities and departmental LCMS facility (supported by DST-FIST grant: SR/FST/CS-I/2018/55) at IIT Ropar are gratefully acknowledged.

Acknowledgment

We thank Mr. Kamlesh Satpute for crystallographic analysis.

Supporting Information

Supporting Information for this article is available online at https://doi.org/10.1055/a-2020-0308.

Conflict of Interest

The authors declare no conflict of interest.

References

(1) Fix, A. G.; Deal, P. E.; Vonnegut, C. L.; Rose, B. D.; Zakharov, L. N.; Haley, M. M. *Org. Lett.* **2013**, *15*, 1362.
(2) (a) Chase, D. T.; Rose, B. D.; McClintock, S. P.; Zakharov, L. N.; Haley, M. M. *Angew. Chem. Int. Ed.* **2011**, *50*, 1127. (b) Shimizu, A.; Tobe, Y. *Angew. Chem. Int. Ed.* **2011**, *50*, 6906. (c) Shimizu, A.; Kishi, R.; Nakano, M.; Shiomi, D.; Sato, K.; Takui, T.; Hisaki, I.; Miyata, M.; Tobe, Y. *Angew. Chem. Int. Ed.* **2013**, *52*, 6076. (d) Dressler, J. J.; Zhou, Z.; Marshall, J. L.; Kishi, R.; Takamuku, S.; Wei, Z.; Spisak, S. N.; Nakano, M.; Petrukhina, M. A.; Haley, M. M. *Angew. Chem. Int. Ed.* **2017**, *56*, 15363. (e) Tobe, Y. *Top. Curr. Chem.* **2018**, *376*, 12. (f) Nishida, J.; Tsukaguchi, S.; Yamashita, Y. *Chem. Eur. J.* **2012**, *18*, 8964. (g) Das, S.; Wu, J. *Phys. Sci. Rev.* **2017**, *2*, 20160109. (h) Casares, R.; Martínez-Pinel, Á.; Rodríguez-González, S.; Márquez, I. R.; Lezama, L.; González, M. T.; Leary, E.; Blanco, V.; Fallaque, J. G.; Díaz, C.; Martín, F.; Cuerva, J. M.; Millán, A. *J. Mater. Chem. C* **2022**, *10*, 11775.
(3) Paudel, K.; Johnson, B.; Thieme, M.; Haley, M. M.; Payne, M. M.; Marcia, M.; Anthony, J. E.; Ostroverkhova, O. *Appl. Phys. Lett.* **2014**, *105*, 043301.
(4) Barker, J. E.; Frederickson, C. K.; Jones, M. H.; Zakharov, L. N.; Haley, M. M. *Org. Lett.* **2017**, *19*, 5312.
(5) (a) Jousselin-Oba, T.; Deal, P. E.; Fix, A. G.; Frederickson, C. K.; Vonnegut, C. L.; Yassar, A.; Zakharov, L. N.; Frigoli, M.; Haley, M. M. *Chem. Asian J.* **2019**, *14*, 1737. (b) Jiang, Q.; Han, Y.; Zou, Y.; Phan, H.; Yuan, L.; Herng, T. S.; Ding, J.; Chi, C. *Chem. Eur. J.* **2020**, *26*, 15613.
(6) (a) Marshall, J. L.; Lehnherr, D.; Lindner, B. D.; Tykwinski, R. R. *ChemPlusChem* **2017**, *82*, 967. (b) Herzog, S.; Hinz, A.; Brehr, F.; Podlech, J. *Org. Biomol. Chem.* **2022**, *20*, 2873.
(7) Sharma, H.; Bhardwaj, N.; Das, S. *Org. Biomol. Chem.* **2022**, *20*, 8071.
(8) Sharma, H.; Sharma, P. K.; Das, S. *Chem. Commun.* **2020**, *56*, 11319.
(9) (a) Lehnherr, D.; Gao, J.; Hegmann, F. A.; Tykwinski, R. R. *Org. Lett.* **2008**, *10*, 4779. (b) Etschel, S. H.; Waterloo, A. R.; Margraf, J. T.; Amin, A. Y.; Hampel, F.; Jäger, C. M.; Clark, T.; Halik, M.; Tykwinski, R. R. *Chem. Commun.* **2013**, *49*, 6725. (c) Zirzlmeier, J.; Lehnherr, D. P.; Coto, B.; Chernick, E. T.; Casillas, R.; Basel, B. S.; Thoss, M.; Tykwinski, R. R.; Guldi, D. M. *Proc. Natl. Acad. Sci. U.S.A.* **2015**, *112*, 5325. (d) Tykwinski, R. R. *Acc. Chem. Res.* **2019**, *52*, 2056.
(10) Ren, L.; Liu, C.; Wang, Z.; Zhu, X. *J. Mater. Chem. C*, **2016**, *4*, 5202.
(11) Hu, P.; Lee, S.; Herng, T. S.; Aratani, N.; Gonçalves, T. P.; Qi, Q.; Shi, X.; Yamada, H.; Huang, K.-W.; Ding, J.; Kim, D.; Wu, J. *J. Am. Chem. Soc.* **2016**, *138*, 1065.
(12) Zeng, W.; Sun, Z.; Herng, T. S.; Gonçalves, T. P.; Gopalakrishna, T. Y.; Huang, K.-W.; Ding, J.; Wu, J. *Angew. Chem. Int. Ed.* **2016**, *55*, 8615.
(13) Yadav, P.; Das, S.; Phan, H.; Herng, T. S.; Ding, J.; Wu, J. *Org. Lett.* **2016**, *18*, 2886.
(14) Sharma, P. K.; Das, S. *J. Org. Chem.* **2022**, *87*, 5430.
(15) Frisch, M. J. et al. Gaussian 09 (*Revision B.01*), (see the Supporting Information for full reference).
(16) Chase, D. T.; Fix, A. G.; Kang, S. J.; Rose, B. D.; Weber, C. D.; Zhong, Y.; Zakharov, L. N.; Lonergan, M. C.; Nuckolls, C.; Haley, M. M. *J. Am. Chem. Soc.* **2012**, *134*, 10349.
(17) Considering *r*(H) 1.1 Å, the F···H distance is still less than Σr_{vdW}. Rowland, R. S.; Taylor, R. *J. Phys. Chem.* **1996**, *100*, 7384.
(18) (a) Desiraju, G. R. *Angew. Chem. Int. Ed.* **2011**, *50*, 52. (b) Champagne, P. A.; Desroches, J.; Paquin, J. *Synthesis* **2015**, *47*, 306.
(19) Karthik, G.; Krushna, P. V.; Srinivasan, A.; Chandrashekar, T. K. *J. Org. Chem.* **2013**, *78*, 8496.
(20) Gopalakrishna, T. Y.; Reddy, J. S.; Anand, V. G. *Angew. Chem. Int. Ed.* **2013**, *52*, 1763.
(21) (a) Haley, M. M. *Chem. Rec.* **2015**, *15*, 1140. (b) Frederickson, C. K.; Rose, B. D.; Haley, M. M. *Acc. Chem. Res.* **2017**, *50*, 977.
(22) Rose, B. D.; Shoer, L. E.; Wasielewski, M. R.; Haley, M. M. *Chem. Phys. Lett.* **2014**, *616*, 137.
(23) Gopalakrishna, T. Y.; Zeng, W.; Lu, X.; Wu, J. *Chem. Commun.* **2018**, *54*, 2186.
(24) (a) Goh, C.; Kline, R. J.; McGehee, M. D.; Kadnikova, E. N.; Fréchet, J. M. J. *Appl. Phys. Lett.* **2005**, *86*, 122110. (b) Thompson, B. C.; Kim, B. J.; Kavulak, D. F.; Sivula, K.; Mauldin, C.; Frechet, J. M. J. *Macromolecules* **2007**, *40*, 7425.
(25) (a) Li, Y.; Clevenger, R. G.; Jin, L.; Kilway, K. V.; Peng, Z. *J. Mater. Chem. C* **2014**, 7180. (b) Blakesley, J.C.; Castro, F. A.; Kylberg, W.; Dibb, G. F. A.; Arantes, C.; Valaski, R.; Cremona, M.; Kim, J.S.; Kim. J.-S. *Org. Electron.* **2014**, *15*, 1263.
(26) Murgatroyd, P. N. *J. Phys. D: Appl. Phys.*, **1970**, *3*, 151.
(27) (a) Blom, P. W. M.; Mihailetchi, V. D.; Koster, L. J. A.; Markov, D. E. *Adv. Mater.* **2007**, *19*, 1551. (b) Yin, H.; Bi, P.; Cheung, S. H.; Cheng, W. L.; Chiu, K. L.; Ho, C. H. Y.; Li, H. W.; Tsang, S. W.; Hao, X.; So, S. K. *Sol. RRL* **2018**, *2*, 1700239.
(28) (a) Chu, T.-Y.; Song, O.-K. *Appl. Phys. Lett.* **2007**, *90*, 203512. (b); Zhang, L.; Xing, X.; Chen, Z.; Xiao, L.; Qu, B.; Gong, Q. *Energy Technol.* **2013**, *1*, 613. (c) Zhou, C.; Chen, Z.; Zhang, G.; McDowell, C.; Luo, P.; Jia, X.; Ford, M. J.; Wang, M.; Bazan, G. C.; Huang, F.; Cao, Y. *Adv. Energy Mater.* **2018**, *8*, 1701668.
(29) Horii, K.; Nogata, A.; Mizuno, Y.; Iwasa, H.; Suzuki, M.; Nakayama, K.-i.; Konishi, A.; Yasuda, M. *Chem. Lett.* **2022**, *51*, 325.
(30) (a) Konishi, A.; Yasuda, M. *Chem. Lett.* **2021**, *50*, 195. (b) Peters, D. *J. Chem. Soc.* **1958**, 1028. (c) Peters, D. *J. Chem. Soc.* **1958**, 1039.
(31) Marshall, J. L.; O'Neal, N. J.; Zakharov, L. N.; Haley, M. M. *J. Org. Chem.* **2016**, *81*, 3674.
(32) Batista, V. S.; Crabtree, R. H.; Konezny, S. J.; Luca, O. R.; Praetorius, J. M. *New J. Chem.* **2012**, *36*, 1141.